Applied Catalysis A, General 545 (2017) 104–112

Contents lists available at ScienceDirect

Applied Catalysis A, General

journal homepage: www.elsevier.com/locate/apcata

Research Paper

Vapor-phase transport (VPT) modification of ZSM-5/SiC foam catalyst using TPAOH vapor to improve the methanol-to-propylene (MTP) reaction

Yilai Jiao[a,c,1], Xiaolei Fan[b,1], Michal Perdjon[c], Zhenming Yang[a], Jinsong Zhang[a,*]

[a] Institute of Metal Research, Chinese Academy of Sciences, 72 Wenhua Road, Shenyang 110016, China
[b] School of Chemical Engineering and Analytical Science, The University of Manchester, Oxford Road, Manchester, M13 9PL, United Kingdom
[c] Cardiff Catalysis Institute, Centre for Doctoral Training in Catalysis, School of Chemistry, Cardiff University, Park Place, Cardiff, CF10 3AT, United Kingdom

ARTICLE INFO

Keywords:
Vapor-phase transport (VPT)
Tetrapropylammonium hydroxide (TPAOH)
ZSM-5
SiC foam
Structured catalyst
Methanol-to-propylene (MTP)
Thermal conductivity

ABSTRACT

Tetrapropylammonium hydroxide (TPAOH) was introduced in the vapor phase to perform the vapor-phase transport (VPT) modification of the structured ZSM-5 supported on SiC foam (ZSM-5/SiC foam) catalyst. An optimum precursor concentration of 0.5 M TPAOH could effectively convert the amorphous aluminosilicate binder to the zeolitic phase with improved intracrystal mesopores, nanosized crystals (*ca.* 100 nm), high concentration of acidity sites (83 mmol g^{-1}) as well as a high value of the relative acidity (0.7). Combined with the intrinsic property of macroscopic SiC foams such as the low pressure drop and the high thermal conductivity (14 W m^{-1} K^{-1} at 773 K), TPAOH VPT modified ZSM-5/SiC foam catalyst demonstrated an excellent activity in the catalytic methanol-to-propylene (MTP) reaction, surpassing the state-of-the-art hierarchal ZSM-5 monolith catalyst. The catalyst showed an extended activity for *ca.* 970 h (> 95% methanol conversion) with the high selectivity to the propylene (> 45%). The coke formation was significantly retarded (*ca.* 2.1 × 10^{-2} wt.% h^{-1}) due to the enhanced transport phenomena within the developed structured catalyst.

1. Introduction

Propylene is a major chemical building block for an array of chemicals and plastics in the modern chemical industry. Propylene is mostly produced (> 30%) as the by-product of the high severity fluid catalytic cracking (HS-FCC, > 823 K) [1], which requires the high catalyst-to-oil ratio (> 20 wt.%) and is highly energy-intensive with low propylene yields (< 20%). On-purpose propylene production routes such as the methanol-to-propylene (MTP) have attracted an increasing attention over the past decades [2–14] thanks to the maturity of syngas-to-methanol processes. In MTP processes, the dehydration reactions occurs within the microporous framework catalysts such as ZSM-5 [2–8,10–14], where the conversion of methanol, the selectivity to propylene as well as the coke formation are greatly influenced by the nature of the acid sites in zeolites and the mass transport through the pore network. As a result, efforts have been made to perform the crystal engineering of ZSM-5 zeolites to optimize the acidity and enhance the molecular transport in their frameworks [12,14] to ensure the kinetic control of MTP reactions. Additionally, the MTP process is exothermic (*ca.* −42 ± 7 kJ mol^{-1}) [13,15] and the poor heat transfer property of the bulk and/or pelleted ZSM-5 (thermal conductivity = *ca.* 0.3 W m^{-1} K^{-1}) can also result in the formation of hot spots along the reaction bed [13] and the associated catalyst deactivation [16]. Therefore, in practical settings, apart from the interparticle mass transfer, the mass transfer of species from the bulk media to the catalyst surface, heat transfer as well as pressure drop need to be accounted for delivering the optimum performance of the process. Accordingly, the optimization of industrial MTP catalyst needs to be addressed as a whole for developing efficient MTP processes at scales [12].

Structured catalysts and reactors are a class of compact technologies [3,5,6,8,11,17–21] that provided an integrated approach for solving the heat and mass transfer challenges in chemical processes. Among structured catalysts, macroscopic cellular ceramic foams, especially silicon carbide (SiC) foams, have archived the popularity for MTP processes due to the intrinsic physical and chemical properties of the foam support materials. For example, SiC has the high thermal conductivity of *ca.* 140 W m^{-1} K^{-1} and low linear expansion coefficient of 2.7 × 10^{-6} K^{-1} [5,6,8,20,22–26]. The SiC cellular open-cell structure also has the geometric properties of high mechanical strength (> 10 MPa), high permeability, low pressure drop and enhanced axial and radial mixing (promoted by the stochastic nature of the interconnected cells) [23,26–31]. Therefore, SiC foams are promising

* Corresponding author.
E-mail address: jshzhang@imr.ac.cn (J. Zhang).
[1] These authors contributed equally to this work.

http://dx.doi.org/10.1016/j.apcata.2017.07.036
Received 25 April 2017; Received in revised form 21 July 2017; Accepted 24 July 2017
Available online 26 July 2017

enablers to bridge the gap between the laboratory development and industrial adoption in the catalytic MTP process by solving the scaling-up issues, which were commonly experienced by the conventional packed-bed (based on zeolite pellets) and monolithic configurations.

As demonstrated in our previous work, structured ZSM-5 supported on SiC foam catalysts (ZSM-5/SiC foam) have shown improved catalytic performance and stability in MTP reactions in comparison to ZSM-5 pellets [3,5,6,8]. In the preparation of the ZSM-5 coating on SiC foams, the structured catalysts were commonly assembled by the direct hydrothermal synthesis [5,25], microwave-assisted synthesis [20] and dip-coating [6]. However, the quality of zeolitic coating in terms of morphology, crystal size and acid properties cannot match that of conventionally prepared bulk zeolites because of the use of amorphous binders and the lack of control in crystal growth on SiC foam surface. Therefore, to improve the quality of the zeolitic coating on SiC foams is crucial to increase the process efficiency of the MTP.

Steaming and vapor-phase transport (VPT) modification were commonly used for the post-synthetic modification of bulk zeolites and self-supporting zeolite membranes by crystalizing the semi-crystalline and/or amorphous precursors. Especially VPT methods, structural directing agents (hazardous amines such as ethylenediamine, EDA and trimethylamine, TEA) were used to facilitate the transformation of aluminosilicate binders to zeolitic phases with the good mechanical strength [12,32,33]. Recently, tetrapropylammonium hydroxide (TPAOH, a less toxic amine than EDA and TEA and the most effective template for formation of Mordenite Framework Inverted-type zeolites, MFI) [7,34,35] was found suitable as the vapor source to increase the relative crystallinity, mesopore volume and Si/Al ratio, and hence the enhanced catalytic stability and selectivity to light olefins [7].

Motivated by the work above, we deduced that VPT modification of ZSM-5/SiC foam using the TPAOH steam could promote the structured catalyst with the improved ZSM-5 coating and the associated catalytic property in the MTP process. ZSM-5/SiC foam catalysts were fabricated by dip coating SiC foam supports with bulk ZSM-5 zeolites using the amorphous aluminosilicate as the binder. Then, TPAOH aqueous solutions were used to generate the vapor to perform the VPT modification of the mixed phase of ZSM-5/aluminosilicate binder on SiC foams. The effect of the TPAOH concentration on the relative crystallinity, mesopore volume, total acidity and ratio of weak acidity to strong acidity were studied in details. The performance of the developed structured catalysts in the MTP process was evaluated under an industrially relevant velocity and also compared with reference catalysts such as steamed ZSM-5/SiC foam catalyst and conventional ZSM-5 pellets.

2. Experimental

2.1. SiC foam supports

SiC foam supports were prepared by the macromolecule pyrogenation combined with the controlled melt infiltrating reaction sintering method [5,6,36]. The as-prepared SiC foam supports possess the open porosity of *ca.* 70% (20 pores per in., PPI) and the open-cell diameter of about 1.3 mm with the compressive strength of about 12 MPa.

2.2. Synthesis of ZSM-5 zeolites

ZSM-5 zeolite was synthesized hydrothermally according to the method reported previously [6]. All chemicals were used as received. The synthesis solution was prepared by mixing tetrapropylammonium hydrate (TPAOH, 50% aqueous solution, China Haohua Chemical Group Co., Ltd) and aluminium chloride ($AlCl_3$, 99.999%, Sinopharm Chemical Reagent Co., Ltd) in deionized water (DW). Colloidal silica (LUDOX® SM colloidal silica, 30 wt%, Sinopharm Chemical Reagent Co., Ltd) was then added in the synthesis solution drop by drop. The final molar composition of the solution is LUDOX®: TPAOH:$AlCl_3$:DW = 1:0.16:0.023:29. The crystallization was conducted in an autoclave reactor (100 cm^3) under hydrostatic conditions at 363 K for 12 h and further reacted at 433 K for 36 h.

2.3. Preparation and vapor-phase transport (VPT) modification of ZSM-5/Sic foam catalysts

ZSM-5/SiC foam catalysts were prepared by dip coating. The aluminosilicate binder was prepared by adding 0.226 g of $AlCl_3$ and 20 g of LUDOX® to 86 cm^3 of DW under vigorous stirring. Then 14 g of the as-prepared bulk ZSM-5 zeolite was added into the solution, followed by the ball milling (at 150 rpm for 4 h, QM-3SP2, Nanjing University Instrument Plant) to form a fine slurry. Dip coating was carried out by: (*i*) immersing SiC foam supports in the slurry for 3–5 min; (*ii*) removing the residual slurry by air blowing; and (*iii*) drying the sample at 313 K for 2 h. The whole process was repeated three times for one sample to ensure the uniform coating of ZSM-5 zeolite on SiC foams (Fig. S1). The loading of ZSM-5 (26 wt%, margin of error = 5%) was estimated by the weight gain of the foam support after the dip coating processes.

The vapor-phase transport (VPT) modification of ZSM-5 coating on SiC foams was carried out in an autoclave reactor with the inner diameter of 80 mm and the depth of 100 mm, provided a capacity of about 500 cm^3. The liquid charged in the autoclave was about 100 cm^3 to avoid the complete vaporization and to maintain the vapor-liquid co-existence in the autoclave at the treatment temperature of 433 K (for 48 h) and autogenous pressure [37]. During the VPT modification, the fresh ZSM-5/SiC foam catalyst was hung about 2 cm above the liquid level (before the heating was applied). Two TPAOH aqueous solutions with the concentration of 0.5 M and 1.0 M were used to generate the alkaline vapor and modify the ZSM-5 coating. After the VPT modification with the TPAOH vapor, the autoclave was cooled down to room temperature naturally, and then catalysts were removed from the autoclave reactor for washing (with DW for three times) and drying (at 383 K overnight). A control experiment of the VPT modification of ZSM-5 coating using the DW vapor was also performed at 433 K. All catalysts, including the untreated one, were calcined at 823 K for 6 h under air to remove the remained organic templates. All ZSM-5 zeolite coatings were converted into the protonated form (HZSM-5) by the ion exchange in aqueous ammonium nitrate solution (1.0 M) at 153 K for 24 h, followed by drying at 383 K (12 h) and calcination at 823 K (6 h), before the characterization and catalytic test.

The denotation of catalysts of S-F, S-DW, S-TPAOH-0.5 and S-TPAOH-1 was used to represent the fresh reference ZSM-5/SiC catalyst, the steamed ZSM-5/SiC catalyst, the 0.5 M TPAOH VPT modified ZSM-5/SiC catalyst and the 1.0 M TPAOH VPT modified ZSM-5/SiC catalyst, respectively.

2.4. Characterization of catalysts

ZSM-5/SiC foams catalysts were characterized by X-ray diffraction (XRD, Rigaku Ultima IV, Japan, Cu*Kα* radiation, 30 kV, 15 mA, λ = 1.5406 Å, 5° < 2θ < 35°, step size = 0.02° and a step time = 2 s) and scanning electron microscopy (SEM, Zeiss SUPRA 35, Germany, 9 kV accelerating voltage) equipped with an energy dispersive X-ray spectrometer (EDX). Prior to the SEM imaging, the sample was coated with gold to avoid the charge effect during the SEM analysis.

The specific surface area and pore structure of the ZSM-5 zeolite coatings was determined by nitrogen (N_2) adsorption–desorption measurements at the liquid nitrogen temperature (77 K) using a Micromeritics 3Flex Surface Characterization Analyzer (Micromeritics, USA). The Si/Al ratio of the ZSM-5 zeolite was determined using the inductively coupled plasma optical emission spectroscopy (ICP-OES, Optima 7300 V HF, USA).

Ammonia temperature-programmed desorption (NH_3-TPD) measurements were performed using a Micromeritics AutoChem II 2920 chemisorption analyzer (Micromeritics, USA) to determine the acidity

and the amount of the acidic sites of the structured zeolite catalysts. The catalyst (400 mg) was pre-treated at 823 K for 1 h and then cooled down to 323 K under Helium (He). A gas mixture of NH_3 in He (10%:90%, 30 $cm^3\ min^{-1}$) was then introduced to saturate the catalyst followed by the purge of pure He (60 $cm^3\ min^{-1}$) at 373 K for 2 h to remove the physically adsorbed NH_3. Finally, NH_3-TPD was performed by heating the catalyst from 373 K to 873 K with a heating rate of 10 K min^{-1} under He flow (30 $cm^3\ min^{-1}$) and the desorbed NH_3 was monitored by a gas chromatography (GC) equipped with a thermal conductivity detector (TCD).

The determination of the coke amount of the spent catalyst was conducted by the thermogravimetry analysis (TGA) performed on a TG analyzer (Pyris Diamond TG/DTA, PerkinElmer) at a heating rate of 300 K min^{-1} from 300 to 1100 K in air (20 $cm^3\ min^{-1}$). The thermal conductivity of materials was evaluated by a transient method using a TPS 2500S Thermal Constants Analyzer (Hot Disk AB, Sweden) according to the standard of ISO 22007-2 [38].

2.5. Catalytic methanol to propylene (MTP) process

The methanol to propylene (MTP) reaction was carried out in a packed column reactor. Methanol (HPLC grade, ≥99.9%, Sinopharm Chemical Reagent Co., Ltd) was used as received. The inner diameter of the column was 26 mm and five pieces of ZSM-5/SiC foam catalyst (pillar foams with the diameter of 25 mm and length of 24 mm) were packed within the column. Thermocouples were placed along the bed at 10 mm interval to monitor the bed temperature. MTP reactions were carried out under conditions of 743 K, 0.1 MPa and methanol weight hourly space velocity (WHSV, defined as the weight of methanol flowing through the catalyst bed per unit weight of the ZSM-5 on SiC foam support per) of 3 h^{-1} (flow rates: $F_{nitrogen}$ = 500–2000 $cm^3\ min^{-1}$, $F_{methanol}$ = 0.61 $cm^3\ min^{-1}$, F_{water} = 0.48 $cm^3\ min^{-1}$). The product distribution of hydrocarbons and dimethylether (including the unreacted methanol) was analyzed by a GC (Agilent 7890A GC) equipped with a PoraPLOT Q column (fused silica ID = 0.32 mm and length = 50 m) and a flame ionization detector (FID). The conversion of methanol ($x_{methanol}$) was calculated according to Eq. (1). The selectivity of the hydrocarbon (S_{C_x}) was calculated on basis of the total hydrocarbons formed as measured in the outlet stream of the reactor (Eq. (2)).

$$x_{methanol} = \frac{C_{methanol,inlet} - C_{methanol,outlet}}{C_{methanol,\ inlet}} \times 100\% \quad (1)$$

$$S_{C_x} = \frac{C_{C_x,outlet}}{C_{C_{total},outlet}} \times 100\% \quad (2)$$

where $C_{methanol,inlet}$ and $C_{methanol,outlet}$ are concentrations of methanol measured by GC analysis at the inlet and outlet of the reactor; $C_{C_x,outlet}$ and $C_{C_{total},outlet}$ are concentrations of the target hydrocarbon and total hydrocarbons at the outlet of the reactor.

3. Results and discussion

3.1. Characterization of ZSM-5/SiC foam catalysts

XRD patterns of materials are shown in Fig. 1. All samples presented similar X-ray diffraction patterns of the MFI structure with the characteristic doublet and triplet peaks at about 7.9 and 8.8° 2θ and 23.1, 24.0 and 24.5° 2θ, respectively. The variation of the peak intensity was obvious at about 8.0 and 8.9° 2θ, especially for TPAOH vapor treated samples, *i.e.* S-TPAOH-0.5 and S-TPAOH-1. Shifts of line positions of ZSM-5 XRD peaks were also noticed for S-TPAOH-0.5 and S-TPAOH-1 in comparison to the fresh and DW treated samples (Table S1). These can be attributed to (*i*) the phase transition of ZSM-5 and (*ii*) the removal of extra framework organic and inorganic species incorporated into the intracrystallines void [39] during the post-synthetic VPT modification using the TPAOH vapor. For ZSM-5 with the MFI

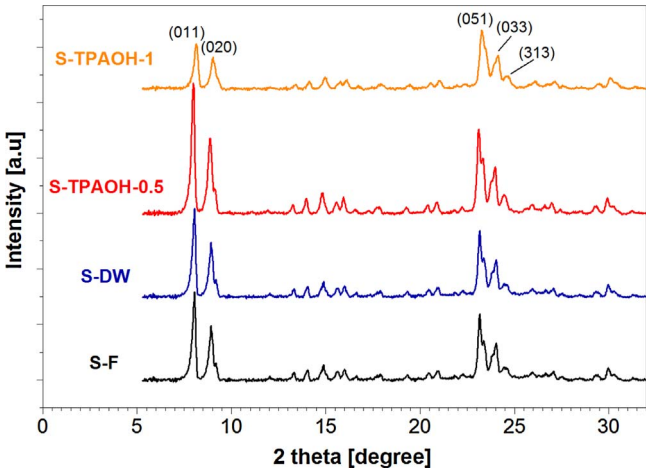

Fig. 1. Powder XRD patterns of ZSM-5 zeolites supported on SiC foams. Miller indices of ZSM-5 were assigned according to reference values obtained from the literature [41].

topology, the 7.9 and 8.8° 2θ doublet corresponds to the monoclinic phase and 22.5–24.5° 2θ corresponds to the orthorhombic phase, respectively [39,40]. The as-synthesized ZSM-5 (after calcination) is known to have the orthorhombic symmetry and the phase change was not found for the DW treated sample by comparing XRD diffractograms of S-F and S-DW. After the VPT modification using 0.5 M TPAOH vapor, S-TPAOH-0.5 showed the monoclinic framework evidenced by the intensity increase of 7.9 and 8.8° 2θ doublet. Interestingly, it was found that an increase in the TPAOH concentration (from 0.5 M to 1.0 M) resulted in the orthorhombic crystal phase again.

The relative crystallinity of zeolite ZSM-5 coating was determined by using the method described in [20]. The comparison of the integrated peak areas in a range of 2θ = 22.5–24.6° was made by using S-TPAOH-0.5 as the reference. It was found that the as-prepared sample (S-F) only had a relative crystallinity of 68.6% due to the use of aluminosilicate binder for coating. After the water vapor VPT, the relative crystallinity of S-DW increased slightly to 73.4%, indicating that the DW vapor has little effect on modifying the coating. The result from the VTP modification using different TPAOH concentrations was quite distinct. S-TPAOH-0.5 catalyst showed the highest relative crystallinity (100%) after the VPT modification with the vapor containing 0.5 M TPAOH, demonstrating that the TPAOH was effective to promote the phase change of aluminosilicate binder (Figs. S2 and S3). However, to increase the TPAOH concentration in the aqueous solution to 1 M, the relative crystallinity of S-TPAOH-1 dropped to 82.9% after the VPT modification. This could be explained by the dissolution and secondary crystallization under highly alkaline conditions which formed new zeolitic phases with a lower relative crystallinity than that of the original ZSM-5.

SEM micrographs of ZSM-5 coating on SiC foams are shown in Fig. 2. For the reference S-F catalyst (Fig. 2a), SiC foam surface was covered by the zeolite/binder mixture, in which zeolite crystal was fully immerged in the amorphous aluminoslicate binder. After being steamed by the DW vapor, no significant changes in the morphology of the mixture were found, as shown in Fig. 2b, which conformed to the result of the XRD analysis as well as to the findings reported in the literature [33]. On the contrary, crystals were formed when TPAOH was introduced to the vapor phase (Fig. 2c and d), which suggested the transformation of the amorphous aluminoslicate into the zeolitic phase. The crystal morphology of the newly formed zeolite (by the TPAOH VPT modification) depends on the concentration of the TPAOH vapor. When 0.5 M TPAOH aqueous solution was used as the vapor source, aggregated nanosized crystals (Fig. 2c) with diameters < 100 nm (Fig. S4a) was formed with morphological features different from the original bulk ZSM-5 crystals used in dip-coating (Fig. S4b). By treating the

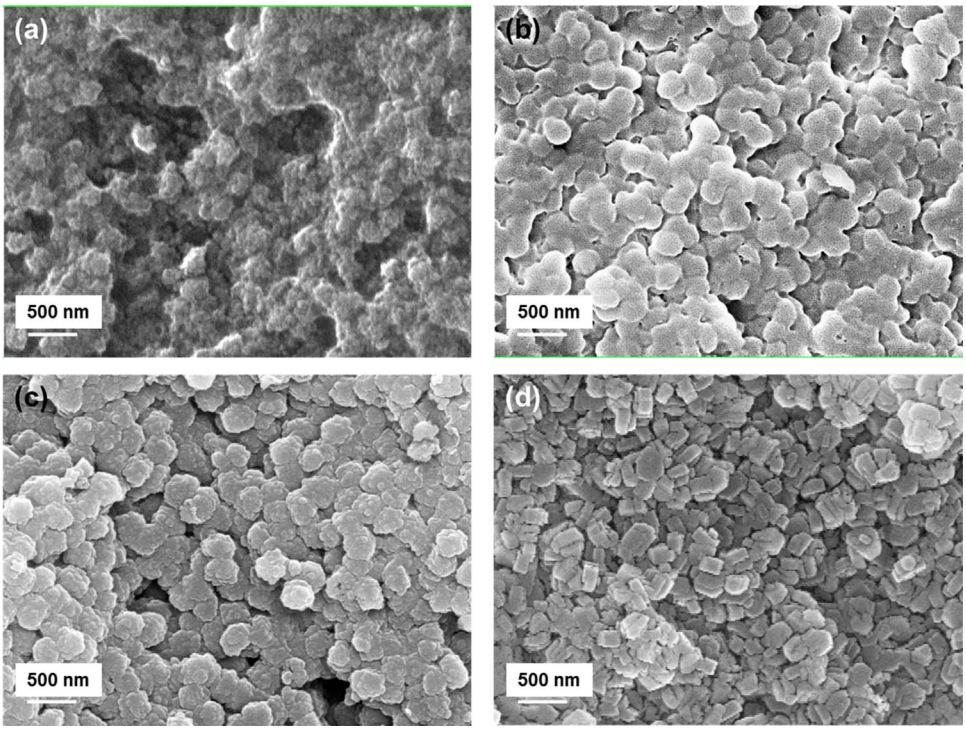

Fig. 2. SEM images of the surface coating of ZSM-5/SiC foam catalysts: (a) S-F catalyst, (b) S-DW catalyst, (c) S-TPAOH-0.5 catalyst and (d) S-TPAOH-1 catalyst.

supported ZSM-5/aluminoslicate mixture using the vapor containing 1.0 M TPAOH, intergrown orthorhombic crystals with sizes of *ca.* 250 nm were formed as shown in Fig. 2d.

N_2 adsorption-desorption isotherms of materials are shown in Fig. 3a. ZSM-5/SiC foam catalysts typically display type IV isotherms with hysteresis loops [42] in a wide relative pressure range of p/p_o = 0.4–0.95. The steaming of ZSM-5 zeolite was commonly carried out at relatively high temperatures (> 673 K) [43] to promote the extraction of the tetrahedral Al to the extraframework position [44]. In this work, the shape of the isotherm of the steamed S-DW was almost identical to that of the untreated sample (S-F), showing that steaming at 443 K did not transform ZSM-5 significantly.

The pore size distribution (PSD, Fig. 3b) was obtain using the non-local density functional theory (NLDFT) [45] based on the adsorption branch of isotherms since the desorption branch was highly likely influenced by the pore network effects [44]. The H3 hysteresis loop suggested the random distribution of pores and the interconnected pore systems [46] in the reference (S-F) and the steamed (S-DW) catalysts. PSDs of S-F and S-DW catalysts show the multimodal distribution with a wide range of pore sizes (centered at around 6 nm), which may be the combination of micropores in ZSM-5 zeolite and mesopores in the aluminosilicate binder phase.

After the VPT modification with the TPAOH vapor at 433 K, N_2 adsorption-desorption isotherms of S-TPAOH-0.5 and S-TPAOH-1 catalysts showed changes in the N_2 uptake and the type of the hysteresis loop, reflecting the change in micro-/meso-pore structures of the coating. In comparison to S-F catalyst, the growth of micropores after alkaline VPT modification was evidenced by the uplifted shoulders at p/p_o = 0.05 (Fig. 3a) and the increased micropore volumes and surfaces (Table 1).

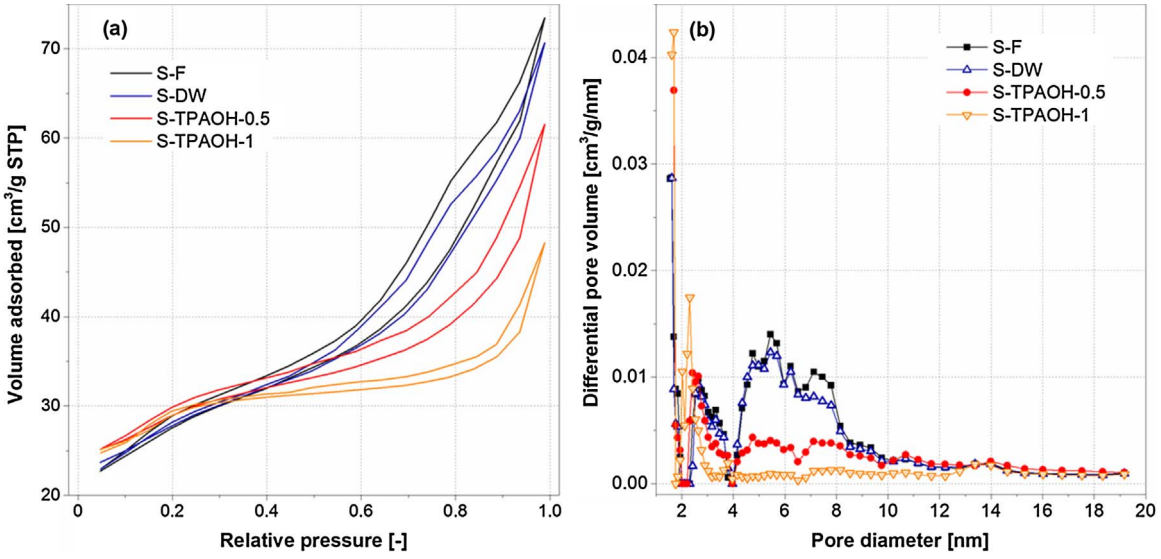

Fig. 3. (a) N_2 adsorption-desorption isotherms at 77 K obtained for ZSM-5/SiC foam catalysts. (b) Pore size distributions of ZSM-5/SiC foams calculated from N_2 adsorption isotherms at 77 K using NLDFT model.

Table 1
Analysis of the N_2 adsorption-desorption data[a] for ZSM-5/SiC foam catalysts.

Catalyst	S_{BET} [$m^2 g^{-1}$]	S_{micro} [$m^2 g^{-1}$]	V_{micro}[b] [$cm^3 g^{-1}$]	V_{BJH}[c] [$cm^3 g^{-1}$]	d_v [nm]
SiC foam[d]	0.4	–	–	–	–
S-F	89	35	1.9×10^{-2}	7.0×10^{-2}	6.4
S-DW	89	38	2.1×10^{-2}	6.5×10^{-2}	6.1
S-TPAOH-0.5	90	51	2.8×10^{-2}	4.2×10^{-2}	3.0
S-TPAOH-1	88	60	3.2×10^{-2}	1.9×10^{-2}	3.7

[a] Data were normalized to the total weight of the relevant materials/composite materials.
[b] Micropore volume was determined according to the *t*-plot method.
[c] V_{BJH} was the Barrett-Joyner-Halenda (BJH) adsorption cumulative volume of pore diameter from 2 to 25 nm.
[d] The external surface area of SiC foam was measured as 5.6×10^{-1} $m^2 g^{-1}$.

The micropore surface and volume of the reference S-F catalyst and the steamed S-DW catalyst are rather similar, whereas that of TPAOH vapor VPT modified catalysts were significantly enhanced, *e.g.* for the micropore surface, by 46% for S-TPAOH-0.5 and 71% for S-TPAOH-1 compared to S-F catalyst, as seen in Table 1. It has been reported that the alkaline VPT modification (with *n*-Butyl amine in the vapor source) could re-crystallize zeolite/binder mixture into new zeolitic phases [12] with modified porous structures. Therefore, the development of the micropore volume and surface area after the TPAOH vapor VPT modification was attributed to the conversion of amorphous aluminosilicate binder into new zeolitic phases under the conditions used (Figs. S2 and S3).

With an increase of the TPAOH concentration to 1 M, the H4 type horizontal hysteresis loop developed gradually for the coating, which is common for the aggregated crystals of zeolites [42]. PSD of S-TPAOH-0.5 still showed the presence of mesopores that could be largely produced in the crystallization process of the aluminosilicate phase, *i.e.* intercrystal pores among the newly formed nano zeolite assembly. The isotherm of S-TPAOH-1 showed a well developed H4 type horizontal hysteresis loop with the adsorption branch close to a composition of Types I and II isotherms [42], indicating the profound micropores creation and the associated intercrystal shrinkage in the secondary crystallization process under an environment with concentrated TPAOH vapor. This also corresponds to PDS of S-TPAOH-1 (Fig. 3b) as well the micropore data in Table 1.

In the VPT modification of zeolite coating, the crystallization is dominated by a dry gel-crystallization mechanism [33,34,47], which was controlled by the alkalinity of the vapor source. When water vapor was used, the lack of the alkalinity in the system could not promote the conversion of amorphous aluminosilicate binder. As an organic amine, TPAOH brought the alkalinity to the vapor phase to promote the diffusion of ionic precursors into the aluminosilicate phase, as well as to stimulate the nucleation as templates within the aluminosilicate binder, allowing the formation of new zeolitic phases with polycrystalline structures. However, the further crystallization could be promoted by the concentrated TPAOH vapor (1 M), leading to the formation of large coffin-like zeolite crystals without the well-developed microporous structures [7,48].

Table 2
Analysis of NH_3-TPD data[a] for ZSM-5/SiC foam catalysts.

Catalyst	*T* of desorption peaks [K]		Weak acid sites [mmol g^{-1}]	Strong acid sites [mmol g^{-1}]	Relative acidity [–]
	First peak	Second peak			
S-F	467	571	14	36	0.4
S-DW	473	576	17	42	0.4
S-TPAOH-0.5	473	584	33	50	0.7
S-TPAOH-1	472	562	26	25	1.0

[a] NH_3-TPD profiles of ZSM-5/SiC foam catalysts are shown in Fig. S5.

NH_3-TPD was performed to assess the amount and strength of acid sites on the developed ZSM-5/SiC foam catalysts. All catalysts showed two desorption peaks of NH_3 (centered at around 470 K and 560–585 K, Fig. S5), which could be associated with the weak acid and strong acid sites, respectively (Table 2). The last column of Table 2 shows the relative acidity (ratio of the weak acidity to the strong acidity). The possession of a high concentration of weak acid sites in ZSM-5 catalysts is very important to enhance the stability of catalysts and increase the propylene selectivity in the MTP process [4,10]. It was found that the TPAOH vapor VPT modification could modify the relative acidity of the catalyst significantly. In comparison with S-F and S-DW catalysts (relative acidity = 0.4), the relative acidity of S-TPAOH-0.5 and S-TPAOH-1 catalysts was increased to 0.7 and 1.0, respectively, implying the enhanced catalytic performance of S-TPAOH-0.5 and S-TPAOH-1 catalysts in the MTP reaction. By a close examination of the amount of acid sites in the S-TPAOH-0.5 and S-TPAOH-1 catalysts, it was noticed that the concentration of weak acid and strong acid sites in S-TPAOH-

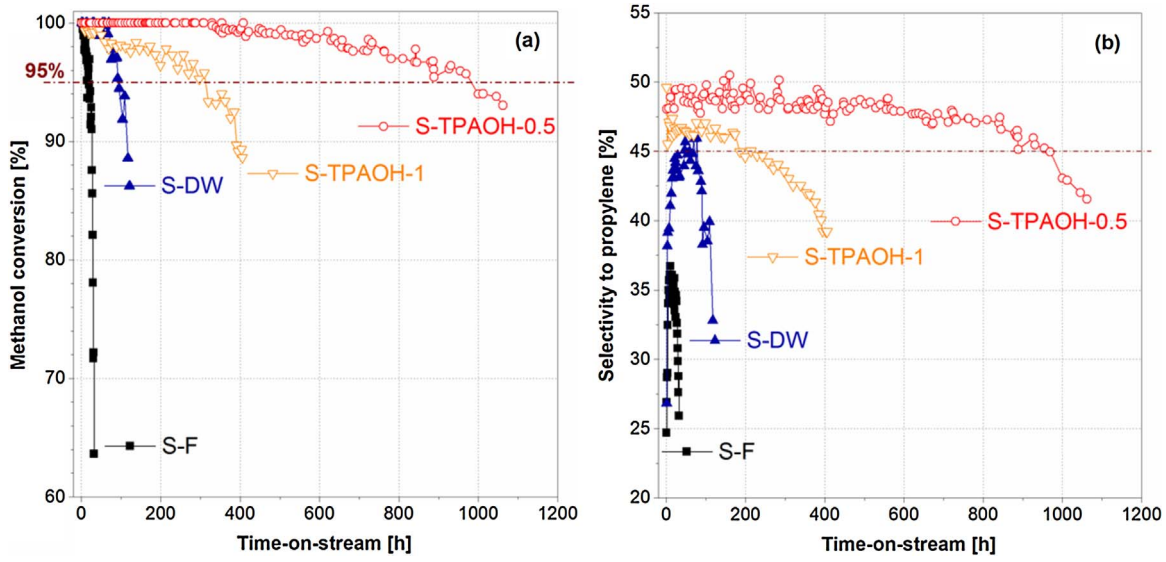

Fig. 4. (a) Methanol conversion and (b) selectivity to propylene as a function of time-on-stream over structured ZSM-5/SiC foam catalysts.

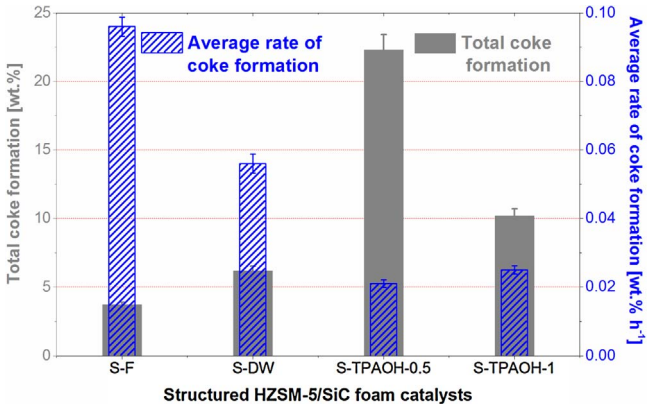

Fig. 5. Coke formation of structured ZSM-5/SiC foam catalysts after MTP reactions.

0.5 catalyst are much higher than that in S-TPAOH-1 catalyst (by 30% and 100% for weak and strong acid sites, respectively), though S-TPAOH-1 catalyst has a higher relative acidity value.

3.2. Methanol to propylene (MTP) process over structured ZSM-5/SiC foam catalysts

The catalytic performance in terms of the methanol conversion and the propylene selectivity of structured ZSM-5/SiC foam catalysts is presented in Fig. 5 as a function of the time-on-stream. S-DW and S-TPAOH-0.5 catalysts showed the high activity with 100% methanol conversion at the initial stage of the reaction (< 20 h), while the initial methanol conversion observed for S-F and S-TPAOF-1 catalysts (*ca.* 96%) were lower than that of the two catalysts above. This could be attributed to the variation of the concentration of strong acid sites in different catalysts (Table 2) since the MTP reaction was initiated by the strong acid sites [4]. It was found that the activity of catalyst with regard to the methanol conversion was affected notably by the post-synthetic VPT modification. For the catalysts obtained by the TPAOH vapor VPT modification (*i.e.* S-TPAOF-0.5 and S-TPAOF-1 catalysts), much better longevities were observed than that of the original (S-F) and steamed catalyst (S-DW). For the catalyst evaluation in the MTP process, a 95% conversion of methanol was commonly used as the benchmark for assessing the activity of a catalyst [12,49], *i.e.* a catalyst was regarded as deactivated on the basis of methanol conversion < 95%. At 743 K, S-F and S-DW catalysts deactivated after about 20 and 40 h time-on-stream, respectively. Comparatively, S-TPAOF-0.5 and S-TPAOF-1 catalysts remained as active for significant long hours, especially S-TPAOF-0.5 catalyst that was active for *ca.* 970 h. S-TPAOF-1 catalyst only showed about 310 h lifetime under the condition used, which would be attributed to its low concentrations of acid sites (Table 2).

The selectivity to propylene (S_{C_3}) of MTP processes based on ZSM-5/SiC foam catalysts is shown in Fig. 4b. In this work, a selective MTP reaction with regard to propylene production was set as $S_{C_3} > 45\%$. Again, in comparison to the original and steamed catalysts, TPAOH vapor VPT modified catalysts showed improved selectivity to propylene. For example, S-TPAOF-0.5 catalyst kept the S_{C_3} value of *ca.* 48% for almost 800 h. Although the value of S_{C_3} for S-TPAOF-1 catalyst is lower than that of S-TPAOF-0.5, the associated MTP process was selective to propylene until 220 h. The product distribution (over different time intervals after start-up) is listed in Table 3. In general, the TPAOH vapor VTP modified catalysts showed noticeable higher selectivity to propylene, while lower selectivities toward light C_1-C_4 alkanes and heavy C_{5+} hydrocarbons than that of S-F and S-DW catalysts. In addition, compared with S-F and S-DW catalysts, the TPAOH treated catalysts also exhibited much higher propylene-to-ethylene ratio (P/E) with an estimated propylene production rate of 148 kg h^{-1} m^{-3} (under steady state for the S-TPAOH-0.5 catalyst). The repeatability of the performance (as the notation e in Table 3 and Fig. S6) and catalyst regeneration (as the notation f in Table 3) were checked for S-TPAOF-0.5 (the standard deviation of the selectivity data is < 2% of the average value).

According to the hydrocarbon-pool mechanism [2,50,51], the production of olefins and cokes under steady state conditions was actually promoted by the reactions between the methanol and hydrocarbon-pool. The carbonaceous species, *i.e.* $(CH_x)_n$ with $0 < x < 2$ [2], in the hydrocarbon-pool were believed to be formed in the induction period of MTP reaction, which can further add reactants and split off products *via* elimination reactions [51]. The hydrocarbon-pool was present in the pores of ZSM-5 and, therefore, the mass transfer steps could affect the activity of zeolite catalysts significantly, *i.e.* enhanced mass transfer could facilitate the transfer of produced olefins back to the bulk media and maintain the activity, whereas trapped products could undergo further reactions such as polymerization, isomerization and aromatization leading to the coke formation and associated deactivation. Therefore, zeolites with hierarchical pore networks and/or nanosized crystals were developed to stimulate the diffusion of MTP products through the porous network of zeolites [9]. Previously, we have showed

Table 3
Product selectivities of structured ZSM-5/SiC foam catalysts catalyzed methanol-to-propylene (MTP) reaction[a].

Catalyst	Time interval [h]	Conversion [%]	Selectivity[b] [%]					P/E [–]
			C_{1-4}	C_2H_4	C_3H_6	C_4H_8	C_{5+}	
S-F	0–10	99.3	8.7	11.4	31.2	19.3	29.2	2.7
S-DW	0–10	100	6.5	9.4	40.0	22.1	22.0	4.3
S-TPAOH-0.5	0–10	100	2.6	9.4	49.0	25.4	13.5	5.2
S-TPAOH-0.5	200–210	100	3.6	7.6	49.3	23.7	15.9	6.5
S-TPAOH-0.5[c]	400–410	99.4	2.8	5.5	48.1	23.0	20.0	8.7
S-TPAOH-0.5	600–610	98.8	2.6	5.0	47.1	21.7	22.5	9.4
S-TPAOH-0.5	880–890	96.3	2.5	5.1	45.8	20.6	22.3	9.1
S-TPAOH-0.5[d]	0–10	99.9	2.8	8.4	49.7	23.9	12.8	5.9
S-TPAOH-0.5[d]	0–10	99.9	2.6	7.3	48.6	24.5	14.3	6.2
S-TPAOH-0.5[e]	0–10	100	2.3	7.8	50.6	25.1	14.2	6.5
S-TPAOH-1	0–10	99.7	3.2	7.9	45.6	25.0	18.0	5.8
S-TPAOH-1	200–210	97.1	2.5	5.6	43.8	22.7	22.4	7.8
S-TPAOH-1	300–310	95.5	2.4	5.0	42.3	21.2	24.7	8.5

[a] WHSV = 3 h^{-1} for all cases.
[b] Carbon mass balance > 95%.
[c] Estimation of the propylene production rate under steady state is about 148 kg h^{-1} m^{-3}.
[d] Repeated experiments for S-TPAOH-0.5 catalyst.
[e] Regeneration experiment for S-TPAOH-0.5 catalyst. The spent catalyst was regenerated by calcination at 823 K under 5 vol.% oxygen in nitrogen for 6 h.

that hierarchically assembled ZSM-5/SiC nanowires/SiC foam catalysts [14] were able to improve the stability (by 550%) and propylene selectivity (by 36%, in comparison to the conventional ZSM-5 pellets [5,6,8]) in MTP by enhancing mass transfers. For S-F and S-DW catalysts, ZSM-5 crystals was mostly surrounded by the amorphous aluminosilicate binder, and hence the retarded diffusion of carbon species from framework to the bulk media could be expected resulting in the relatively poor activity and selectivity as shown in Fig. 4. Although mesopores were measured for the two catalysts by N_2 adsorption-desorption analysis (Fig. 2 and Table 1), they were essentially the mesoscopic voids within the binder phase, not beneficial to MTP reactions.

The amorphous aluminosilicate binder was found converted by the 0.5 M TPAOH vapor to the zeolitic phase with nanosized crystals of < 100 nm (Fig. S3) and the intercrystal mesopores. Therefore, the newly formed nanosized ZSM-5 coating along with the developed hierarchical meso-/micro-pore system in S-TPAOH-0.5 catalyst were favorable to extend the catalytic lifetime of the structured catalyst as well as increase the selectivity to propylene. As discussed above, the increased alkalinity of the vapor phase could facilitate the secondary crystallization and the close of interparticle mesopores (as evidenced by the SEM and N_2 adsorption analysis, Figs. 2 and 3). It was also reported that the selectivity to lower olefins (including propylene) and the catalyst lifetime were decreased when orthorhombic ZSM-5 zeolites were used in MTP reactions instead of monoclinic ZSM-5 zeolites [52]. Hence, S-TPAOH-1 catalyst with zeolite crystals of *ca.* 250 nm and the orthorhombic shape demonstrated unsatisfactory performance in comparison with that of S-TPAOH-0.5 catalyst.

In addition to the change in the morphological and porous features of the zeolitic coating, the enhanced catalytic performance of S-TPAOH-0.5 catalyst can also be explained by the variation of acidity sites of the catalyst after VPT treatment. In MTP reactions, both strong and weak acid sites are regarded as the active sites for promoting the reaction [4,53–55], in which strong acidity initiates MTP reaction and contributes to the conversion of methanol [53] and weak acidity catalyzes reactions of alkylation [55] and methylation [54] for olefin formation. However, the aromatization of olefin is also catalyzed by strong acid sites [53], leading to the coke formation and deactivation. On the other hand, weak acid sites show a better anti-coking capability than the strong ones because weak acid sites do not favor hydrogen-transfer reactions to produce heavy saturated aliphatics and aromatics [55]. Accordingly, both the total concentration of acidity sites and the relative acidity (ratio of weak acidity to strong acidity) are important parameters for the design of zeolite catalysts for an enhanced MTP process [4,10,56].

According to the NH_3-TPR analysis, S-TPAOH-0.5 catalyst has the highest concentration of total acidity sites (83 mmol g^{-1}) among all catalysts studied in this work, as well as a high relative acidity of 0.7. Both were beneficial to the formation of propylene and avoid secondary reactions. For S-TPAOH-1 catalyst, though the highest relative acidity (1.0) was obtained, the total acidity sites are rather low (51 mmol g^{-1}), explained its performance in terms of selectivity and longevity in the MTP reaction. Contrary to the catalysts modified by TPAOH vapors, S-F and S-DW catalysts showed low values in the relative acidity (*ca.* 0.4). Therefore, the coke formation as well as the quick deactivation could be anticipated as seen in Fig. 4a.

TG analysis was carried out to quantify the coke formation of the catalysts used in this study, as shown in Fig. 5. Catalysts were analyzed after the total time-on-stream after MTP reactions. It was found that the amount of coke formed was linked to the total time-on-stream. S-TPAOH-0.5 catalyst was used for long hours, and hence showed the highest value of coke amount of 22 wt.% compared to other three catalysts, *i.e.* 10 wt.% for S-TPAOH-1, 6.2 wt.% for S-DW and 3.7 wt.% for S-F, respectively. However, by considering the average rate of coke formation (*i.e.* the total amount of cokes divided by the total time-on-stream), S-TPAOH-0.5 catalyst demonstrated the best performance (only about 2.1×10^{-2} wt.% h^{-1}).

3.3. MTP process enhancement by SiC foam supports

S-TPAOH-0.5 catalyst with the optimum performance in this study was also compared to the state-of-the-art ZSM-5 catalysts. A hierarchical full-zeolitic monolithic catalyst (ZSM-5) was recently developed by an amine steam-assisted transformation method [12] and showed the longest catalyst life so far for MTP reactions, *i.e.* about 2000 h at 753 K, and three times as long as that of a commercial ZSM-5 catalyst. However, the reaction was carried out at relatively low WHSV of 0.7 h^{-1} with relatively low selectivities to propylene, *i.e.* < 40%. In this work, a high WHSV of 3 h^{-1} was used with the foam based catalyst and the selectivity to propylene was maintained as > 48% for about 800 h (S-TPAOH-0.5 catalyst). The methanol mass converted per unit mass of the zeolite catalyst before the deactivation was calculated in order to compare the catalytic performance of difference catalysts quantitatively. For the ZSM-5 monolith, the weight of converted methanol was about 1.4×10^3 $g_{methanol}/g_{catalyst}$, while it was about 2.9×10^3 $g_{methanol}/g_{catalyst}$ for S-TPAOH-0.5 catalyst. Since both structured catalysts were believed to benefit from the improved mass transfer steps at both inter-crystalline and intra-crystalline scales, the better catalytic performance of the ZSM-5/SiC foam catalyst could be the result of the intrinsic properties of macroscopic SiC foam supports.

The effect of N_2 flow rate on the selectivity to propylene and ethylene of ZSM-5/SiC foam and ZSM-5 pellet catalysts was shown in Fig. 6a. In MTP processes, N_2 carrier gas was used to adjust the partial pressure of methanol, as well as to remove the heat from the reaction due to the exothermic nature of the reaction. Fig. 6a shows that, for the structured ZSM-5/SiC foam catalyst (S-TPAOH-0.5), the effect of N_2 flow rate on the selectivity to ethylene and propylene was less important than that of conventional ZSM-5 pellets. This could be assigned to the low pressure drop and high thermal transport properties of SiC foam supports. The pressure drops across the ZSM-5/SiC foam catalyst bed were measured only as one fifth of the pressure drop of the ZSM-5 pellet catalyst. Therefore, a low pressure drop through the foam bed benefited the shift of reaction equilibrium towards the production of gaseous olefins. Moreover, in comparison to the species transport within the pelleted ZSM-5, the thin ZSM-5 coating layer on SiC foams could further reduce the diffusion path benefiting the production of the propylene.

The measured temperature of different catalyst beds (*i.e.* ZSM-5/SiC foam, SiC pellets diluted ZSM-5 pellets and pure ZSM-5 pellets bed) as a function of bed length at $F_{nitrogen}$ = 1500 cm^3 min^{-1} are presented in Fig. 6b. Apparently, the use of SiC foams as the catalyst support promoted a more uniform temperature distribution with the average bed temperature of 762 ± 3 K compared to the pure ZSM-5 pellet packed bed (779 ± 11 K). The adiabatic temperature rise (ΔT_{ad}) was also reduced by the presence of SiC foam, ΔT_{ad} = 10 K for ZSM-5/SiC foam catalyst *versus* ΔT_{ad} = 31 K for the ZSM-5 pellets. Though the dilution of ZSM-5 pellets bed catalysts bed with SiC pellets could increase the heat transfer through the bed, the initial temperature rise of 17 K was still measured (the average bed temperature of ZSM-5 pellets/SiC pellets bed was 770 ± 5 K). We believe that the intrinsic natures of the ZSM-5/SiC foam catalyst have resulted in the measured temperature gradient along the bed. The open-cell structure facilitated the fluid flow through the foam bed, which promoted the convective heat transfer along the bed. In the conventional packed bed, by contrast, the heat released by the reaction was prone to accumulate within the bed forming hot spot (as the drastic temperature rise in the zeolite pellets bed in Fig. 6b). In the ZSM-5/SiC foam catalyst, the active phase was coated on the SiC support as thin layers. Therefore, the heat released by the reaction should be easily transferred to the bulk fluid media as well as to the SiC support. Whilst, in the packed with the zeolite pellets, heat transfer was limited. Additionally, the high thermal conductivity and interconnected 3D structure ensured an effective heat conduction [23] contributing to the dissipation of heat (through the reactor wall). Therefore, in comparison with a conventional pelleted zeolite bed, the

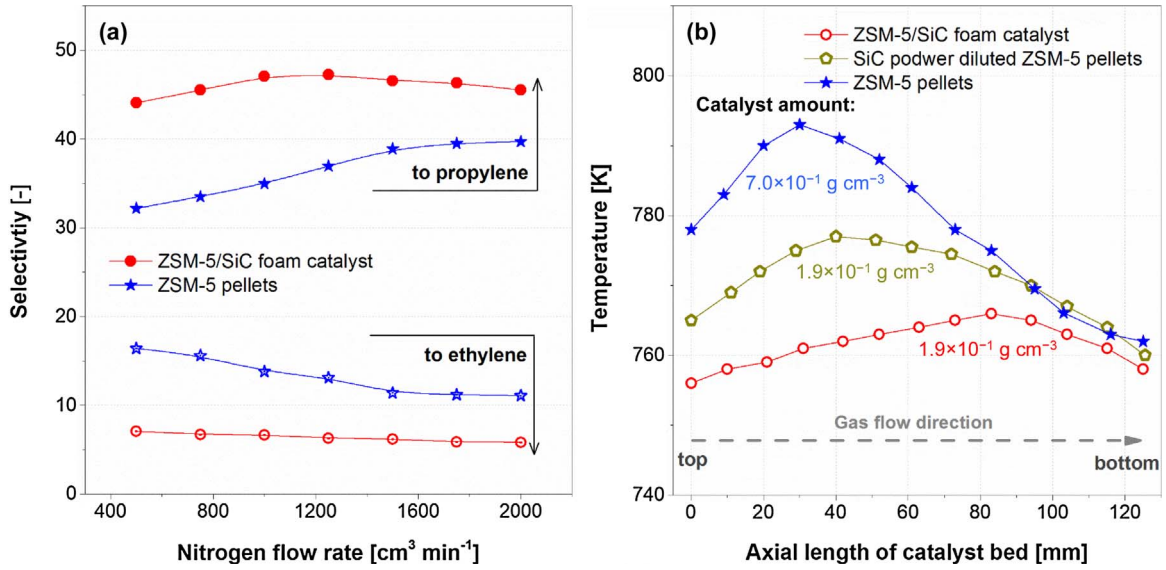

Fig. 6. (a) Steady-state selectivities to propylene and ethylene of ZSM-5/SiC foam and pelleted ZSM-5 catalysts; (b) Steady-state temperature profiles of MTP catalyst beds as a function of the reactor length ($F_{nitrogen}$ = 1500 $cm^3\ min^{-1}$). Catalysts: 50 cm^3 structured ZSM-5/SiC foam catalyst (conversion = 100%); 50 cm^3 ZSM-5 pellets (9.6 g, 0.5 mm diameter, conversion = 95%) diluted by SiC pellets (1.5 mm diameter); 50 cm^3 pure ZSM-5 pellets (35 g, 0.5 mm diameter, conversion = 100%). Conditions: $F_{methanol}$ = 0.61 $cm^3\ min^{-1}$, F_{water} = 0.48 $cm^3\ min^{-1}$, T = 743 K. All data were measured after 5 h of time-on-stream.

maximum temperature gradient of the SiC foam bed was less significant. Similar phenomenon was also measured in oxidative coupling of methane reaction using Na_2WO_4-Mn/SiC monolithic foam catalyst [57]. Additionally, by comparing the different beds, the variation of the contact time through the structured foam catalysts might also play a role in the high stability exhibited by the S-TPAOH catalysts.

The excellent heat transfer property of SiC foams was confirmed by the measurement of the thermal conductivity of materials (λ). As seen in Fig. 7, SiC foams used in this work have the high thermal conductivity that varies in an exponential decay manner with an increase in temperatures. However, the measured intrinsic values of $\lambda_{SiCfoam}$, were at least one order of magnitude higher than that reported in literatures (*i.e.* < 1 $W\ m^{-1}\ K^{-1}$) [16,23]. A slight decrease in λ (by 11 ± 1%) was measured for materials after the coating of ZSM-5 on SiC foam support. At the temperature of MTP process of 773 K, the thermal conductivity of ZSM-5/SiC foam catalyst was still about 14 $W\ m^{-1}\ K^{-1}$, more than 30 times higher than that of SiC pellet diluted zeolite pellets bed (*ca.* 0.4 $W\ m^{-1}\ K^{-1}$).

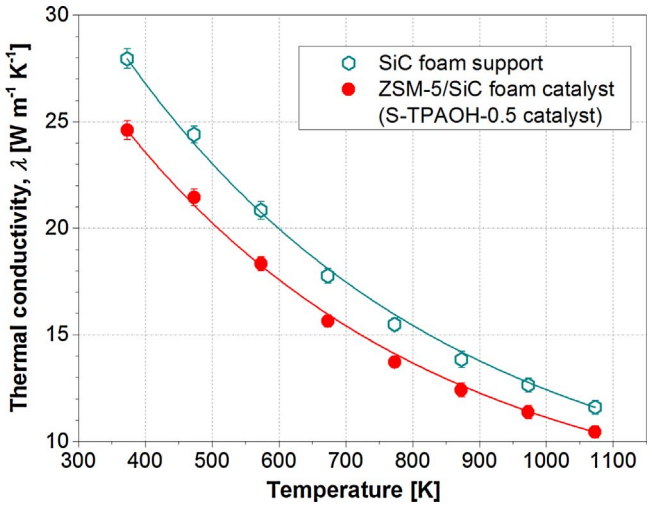

Fig. 7. Thermal conductivity (λ) of SiC foam and ZSM-5/SiC foam catalyst (S-TPAOH-0.5).

4. Conclusion

In conclusion, structured ZSM-5 supported on SiC foam catalysts (ZSM-5/SiC foam) were prepared by dip coating with ZSM-5 in aluminosilcate binder slurry and subsequently modified using the vapor-phase transport (VPT) method with the TPAOH vapor. We demonstrated that TPAOH vapor VPT modification of ZSM-5/SiC foam catalysts could enhance the catalytic performance in the methanol-to-propylene (MTP) process. It was found that VPT modification with 0.5 M TPAOH promoted the effective conversion of amorphous aluminosilcate binder to zeolitic phase with intracrystal mesopores, nanosized crystals (*ca.* 100 nm), high concentration of acidity sites (83 mmol g^{-1}) as well as a high relative acidity (0.7). These features promoted (*i*) the removal of the intermediate products, particularly propylene, from the hydrocarbon-pool in the ZSM-catalyst and (*ii*) a low average coking rate 2.1 × 10^{-2} wt.% h^{-1}). Accordingly, the improved longevity (970 h) and selectivity to propylene (*ca.* 48%), outperformed other catalysts studied in this work. By further increasing the alkalinity of the vapor (with 1 M TPAOH aqueous solution), adverse effects on the zeolitic phase were noticed such as reduced total acidity sites and close-up of intracrystal mesopores, and consequently, a decreased catalytic performance.

The structured ZSM-5/SiC foam catalyst is a technical leap beyond the state-of-the-art ZSM-5 catalyst, *i.e.* a hierarchical pure ZSM-5 monolith. Compared to the monolithic catalyst, the SiC foam based catalyst (after TPAOH vapor VPT modification) showed superior catalytic performance in terms of the methanol conversion per unit mass of catalyst before deactivation, *i.e.* 2.9 × 10^3 $g_{methanol}/g_{catalyst}$ for ZSM-5/SiC foam catalyst *versus* 1.4 × 10^3 $g_{methanol}/g_{catalyst}$ for ZSM-5 monolith catalyst. For MTP processes, macroscopic SiC foams provided low pressure drop (one fifth of that from packed zeolite pellets) as well as high heat transfer property (high thermal conductivity of 14 $W\ m^{-1}\ K^{-1}$ at 773 K) ensured a good selectivity to propylene and uniform bed temperature during operation.

Acknowledgements

The authors would like to thank the financial support from the National 863 Program of China (2012AA030304). XF gratefully acknowledge financial support from the Engineering and Physical

Sciences Research Council for his research (EP/R000670/1) in SiC foam based catalysts. YJ thanks the China Scholarship Council (CSC) for his fellowship in the UK (201604910181). XF and YL also thanks the Higher Education Innovation Funded 'Knowledge and Innovation Hub for Environmental Sustainability' at The University of Manchester for supporting YJ's visit to The University of Manchester.

References

[1] R.S. Parthasarathi, S.S. Alabduljabbar, Appl. Petrochem. Res. 4 (2014) 441–444.
[2] M. Stöcker, Microporous Mesoporous Mater. 29 (1999) 3–48.
[3] F.C. Patcas, J. Catal. 231 (2005) 194–200.
[4] Y. Yang, C. Sun, J. Du, Y. Yue, W. Hua, C. Zhang, W. Shen, H. Xu, Catal. Commun. 24 (2012) 44–47.
[5] Y. Jiao, C. Jiang, Z. Yang, J. Zhang, Microporous Mesoporous Mater. 162 (2012) 152–158.
[6] Y. Jiao, C. Jiang, Z. Yang, J. Liu, J. Zhang, Microporous Mesoporous Mater. 181 (2013) 201–207.
[7] Y. He, M. Liu, C. Dai, S. Xu, Y. Wei, Z. Liu, X. Guo, Chin. J. Catal. 34 (2013) 1148–1158.
[8] Y. Jiao, X. Yang, C. Jiang, C. Tian, Z. Yang, J. Zhang, J. Catal. 332 (2015) 70–76.
[9] Z. Li, J. Martínez-Triguero, J. Yu, A. Corma, J. Catal. 329 (2015) 379–388.
[10] F. Yaripour, Z. Shariatinia, S. Sahebdelfar, A. Irandoukht, Microporous Mesoporous Mater. 203 (2015) 41–53.
[11] J. Ding, Z. Zhang, L. Han, C. Wang, P. Chen, G. Zhao, Y. Liu, Y. Lu, RSC Adv. 6 (2016) 48387–48395.
[12] J. Zhou, J. Teng, L. Ren, Y. Wang, Z. Liu, W. Liu, W. Yang, Z. Xie, J. Catal. 340 (2016) 166–176.
[13] I. Yarulina, F. Kapteijn, J. Gascon, Catal. Sci. Technol. 6 (2016) 5320–5325.
[14] P. Losch, A.B. Pinar, M.G. Willinger, K. Soukup, S. Chavan, B. Vincent, P. Pale, B. Louis, J. Catal. 345 (2017) 11–23.
[15] P. Kumar, J.W. Thybaut, S. Svelle, U. Olsbye, G.B. Marin, Ind. Eng. Chem. Res. 52 (2013) 1491–1507.
[16] L. Borchardt, N.-L. Michels, T. Nowak, S. Mitchell, J. Pérez-Ramírez, Microporous Mesoporous Mater. 208 (2015) 196–202.
[17] M.M. Elamin, O. Muraza, Z. Malaibari, H. Ba, J.-M. Nhut, C. Pham-Huu, Chem. Eng. J. 274 (2015) 113–122.
[18] X. Fan, V. Sans, S.K. Sharma, P.K. Plucinski, V.A. Zaikovskii, K. Wilson, S.R. Tennison, A. Kozynchenko, A.A. Lapkin, Catal. Sci. Technol. 6 (2016) 2387–2395.
[19] C. Duong-Viet, H. Ba, Z. El-Berrichi, J.-M. Nhut, M.J. Ledoux, Y. Liu, C. Pham-Huu, New J. Chem. 40 (2016) 4285–4299.
[20] X. Ou, S. Xu, J.M. Warnett, S.M. Holmes, A. Zaheer, A.A. Garforth, M.A. Williams, Y. Jiao, X. Fan, Chem. Eng. J. 312 (2017) 1–9.
[21] M. Bracconi, M. Ambrosetti, M. Maestri, G. Groppi, E. Tronconi, Chem. Eng. J. 315 (2017) 608–620.
[22] H. Ba, Y. Liu, X. Mu, W.-H. Doh, J.-M. Nhut, P. Granger, C. Pham-Huu, Appl. Catal. A: Gen. 499 (2015) 217–226.
[23] X. Fan, X. Ou, F. Xing, G.A. Turley, P. Denissenko, M.A. Williams, N. Batail, C. Pham, A.A. Lapkin, Catal. Today 278 (Part 2) (2016) 350–360.
[24] S. Ivanova, C. Lebrun, E. Vanhaecke, C. Pham-Huu, B. Louis, J. Catal. 265 (2009) 1–7.
[25] Y. Liu, S. Podila, D.L. Nguyen, D. Edouard, P. Nguyen, C. Pham, M.J. Ledoux, C. Pham-Huu, Appl. Catal. A: Gen. 409–410 (2011) 113–121.
[26] X. Ou, X. Zhang, T. Lowe, R. Blanc, M.N. Rad, Y. Wang, N. Batail, C. Pham, N. Shokri, A.A. Garforth, P.J. Withers, X. Fan, Mater. Charact. 123 (2017) 20–28.
[27] P. Ciambelli, V. Palma, E. Palo, Catal. Today 155 (2010) 92–100.
[28] X. Gao, X. Li, X. Liu, H. Li, Z. Yang, J. Zhang, Chem. Eng. Sci. 135 (2015) 489–500.
[29] H. Li, L. Fu, X. Li, X. Gao, AIChE J. 61 (2015) 4509–4516.
[30] H. Li, F. Wang, C. Wang, X. Gao, X. Li, Chem. Eng. Sci. 123 (2015) 341–349.
[31] V. Palma, A. Ricca, P. Ciambelli, Catal. Today 216 (2013) 30–37.
[32] M. Matsukata, N. Nishiyama, K. Ueyama, J. Chem. Soc. Chem. Commun. (1994) 339–340.
[33] J. Dong, E.A. Payzant, M.Z.C. Hu, D.W. Depaoli, Y.S. Lin, J. Mater. Sci. 38 (2003) 979–985.
[34] N. Nishiyama, K. Ueyama, M. Matsukata, Microporous Mesoporous Mater. 7 (1996) 299–308.
[35] A. Chatterjee, J. Mol. Catal. A: Chem. 120 (1997) 155–163.
[36] W. Wei, X. Cao, C. Tian, J. Zhang, Microporous Mesoporous Mater. 112 (2008) 521–525.
[37] M.B. Yue, M.N. Sun, F. Xie, D.D. Ren, Microporous Mesoporous Mater. 183 (2014) 177–184.
[38] ISO 22007-2, International Organization for Standardization, Switzerland, 2008.
[39] E.L. Wu, S.L. Lawton, D.H. Olson, A.C. Rohrman, G.T. Kokotailo, J. Phys. Chem. 83 (1979) 2777–2781.
[40] F. Jin, X. Wang, T. Liu, Y. Wu, L. Xiao, M. Yuan, Y. Fan, Chin. J. Chem. Eng. (2016), http://dx.doi.org/10.1016/j.cjche.2016.11.004.
[41] H. van Koningsveld, J.C. Jansen, H. van Bekkum, Zeolites 10 (1990) 235–242.
[42] M. Thommes, K. Kaneko, A.V. Neimark, J.P. Olivier, F. Rodriguez-Reinoso, J. Rouquerol, K.S.W. Sing, Pure Appl. Chem. 87 (2015) 1051–1069.
[43] J. Pérez-Ramírez, F. Kapteijn, J.C. Groen, A. Doménech, G. Mul, J.A. Moulijn, J. Catal. 214 (2003) 33–45.
[44] J.C. Groen, L.A.A. Peffer, J. Pérez-Ramírez, Microporous Mesoporous Mater. 60 (2003) 1–17.
[45] ISO 15901-3, International Organization for Standardization, Switzerland, 2007.
[46] K.S.W. Sing, D.H. Everett, R.A.W. Haul, L. Moscou, R.A. Pierotti, J. Rouquerol, T. Siemieniewska, Pure Appl. Chem. 57 (1985) 603–619.
[47] A. Iwasaki, M. Hirata, I. Kudo, T. Sano, S. Sugawara, M. Ito, M. Watanabe, Zeolites 15 (1995) 308–314.
[48] B. Wang, M. Lin, X. Peng, B. Zhu, X. Shu, RSC Adv. 6 (2016) 44963–44971.
[49] S. Zhang, Y. Gong, L. Zhang, Y. Liu, T. Dou, J. Xu, F. Deng, Fuel Process. Technol. 129 (2015) 130–138.
[50] I.M. Dahl, S. Kolboe, J. Catal. 149 (1994) 458–464.
[51] W. Wang, Y. Jiang, M. Hunger, Catal. Today 113 (2006) 102–114.
[52] C.G. Yang, Design and Synthesis of the Catalysts for Methanol-to-olefins (PhD thesis), Jilin University, Jilin, China 2013.
[53] J. Liu, C. Zhang, Z. Shen, W. Hua, Y. Tang, W. Shen, Y. Yue, H. Xu, Catal. Commun. 10 (2009) 1506–1509.
[54] W. Wu, W. Guo, W. Xiao, M. Luo, Chem. Eng. Sci. 66 (2011) 4722–4732.
[55] Q. Zhu, J.N. Kondo, T. Setoyama, M. Yamaguchi, K. Domen, T. Tatsumi, Chem. Commun. (2008) 5164–5166.
[56] Y. Gao, B. Zheng, G. Wu, F. Ma, C. Liu, RSC Adv. 6 (2016) 83581–83588.
[57] H. Liu, D. Yang, R. Gao, L. Chen, S. Zhang, X. Wang, Catal. Commun. 9 (2008) 1302–1306.